

Observation of universal dissipative dynamics in strongly correlated quantum gas

Yajuan Zhao,^{1,*} Ye Tian,^{1,*} Jilai Ye,^{1,*} Yue Wu,² Zihan Zhao,¹ Zhihao Chi,¹
Tian Tian,¹ Hepeng Yao,³ Jiazhong Hu,^{1,4,†} Yu Chen,^{5,‡} and Wenlan Chen^{1,4,§}

¹*Department of Physics and State Key Laboratory of Low Dimensional
Quantum Physics, Tsinghua University, Beijing, 100084, China*

²*Institute for Advanced Study, Tsinghua University, Beijing, 100084, China*

³*DQMP, University of Geneva, 24 Quai Ernest-Ansermet, CH-1211 Geneva, Switzerland*

⁴*Frontier Science Center for Quantum Information and Collaborative
Innovation Center of Quantum Matter, Beijing, 100084, China*

⁵*Graduate School of China Academy of Engineering Physics, Beijing, 100193, China*

(Dated: September 20, 2023)

Dissipation is unavoidable in quantum systems. It usually induces decoherences and changes quantum correlations. To access the information of strongly correlated quantum matters, one has to overcome or suppress dissipation to extract out the underlying quantum phenomena. However, here we find an opposite effect that dissipation can be utilized as a powerful tool to probe the intrinsic correlations of quantum many-body systems. Applying highly-controllable dissipation in ultracold atomic systems, we observe a universal dissipative dynamics in strongly correlated one-dimensional quantum gases. The total particle number of this system follows a universal stretched-exponential decay, and the stretched exponent measures the anomalous dimension of the spectral function, a critical exponent characterizing strong quantum fluctuations of this system. This method could have broad applications in detecting strongly correlated features, including spin-charge separations and Fermi arcs in quantum materials.

Open quantum systems and non-Hermitian physics are emerging topics in recent years, uncovering fascinating dissipation-driven phenomena and attracting considerable attention [1–4]. Ultracold atomic gases are among the best testbeds for exploring dissipation effects in quantum many-body systems because of the full control of both dissipation channels and their strengths, together with the versatile tunability of many-body quantum correlations. Utilizing these advantages, novel physics different from those in closed systems have been observed in cold atom platforms, including dissipative-stabilized strong-correlated matters [5–8], quantum phase transitions in superradiance [9–13], continuous time crystals [14, 15], and dissipation-enabled entangled states [16, 17]. However, these novel physics usually emerge in the strong dissipation regimes and dissipation-driven steady states. In contrast, in the weak dissipation regime and the short-time scale before reaching the steady state, how dissipation interplays with quantum many-body correlations is rarely studied.

A weak dissipation usually does not disturb intrinsic quantum correlations at short time. However, it does cause a dynamical response, usually manifested as the decay of a physical observable in time. With constant dissipation, we often observe exponential decay for most conventional quantum states. These states are quantum phases with well-defined quasi-particles, displaying delta-function type single-particle spectral function. In contrast, if quantum fluctuation in the system is so strong that it destroys well-defined quasi-particles, the dissipative dynamics is predicted to display a stretched-exponential decay [18]. Especially for quantum critical states [19–22], the spectral function ex-

hibits a power-law divergence around the threshold Δ in the form of $(\omega^2 - \Delta^2)^{-\eta}$, and the dissipative dynamics at short time follows a stretched-exponential form of $\exp[-(t/\tau_0)^{2\eta-1}]$ [18]. The power η in the spectral function is the anomalous dimension, a critical exponent manifesting strong quantum fluctuations in this system. Usually, the stronger the quantum fluctuation, the smaller the anomalous dimension η . Thus, measuring the dynamics under weak dissipation provides an alternating route to access many-body correlations at equilibrium, in contrast to existing measurements in condensed matter and cold atom physics using Hermitian perturbation as a probing tool.

The one-dimensional (1D) Bose gas is an optimal choice for performing measurements of strong correlation effects by using dissipation. First, 1D systems are known to display strong quantum fluctuations at low temperature and obey the divergent single-particle spectral function mentioned above [20, 21]. Moreover, its anomalous dimension is tunable by tuning interaction strength [20]. Secondly, the 1D Bose gas is integrable, and the analytical solution allows a quantitative comparison between theory and experiment. This advantage allows us to benchmark this new measurement scheme. Thirdly, 1D atomic gas can be precisely controlled, and many fascinating phenomena have been observed already [23–38]. However, all existing experiments focus on density distributions, momentum distributions, or density and spin correlation functions. The measurement of single-particle spectral function is still missing. Especially, the crucial quantity of the anomalous dimension has not been experimentally measured.

In our experiment, we realize Luttinger liquid of

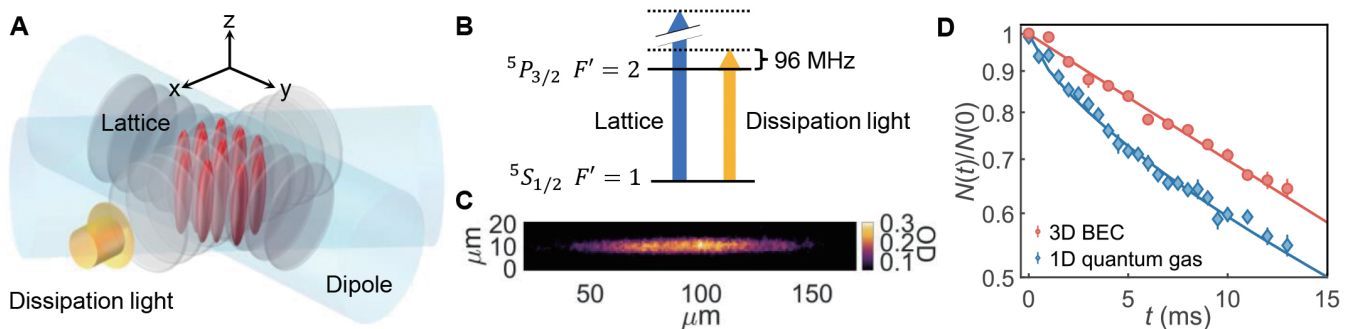


FIG. 1. **Illustration of the experiment setup.** (A), A BEC with 4×10^4 ^{87}Rb atoms is prepared in a crossed dipole trap and loaded into 2D optical lattice made from two orthogonal laser beams. 3300 tubes of 1D Bose gas ensemble are created. A near-resonant light along the x axis is shined onto the ensemble to introduce one-body dissipation. An absorption imaging is set up along the x axis. (B), The dissipation light is set to 96 MHz blue-detuned from $|5S_{1/2}, F=1\rangle \rightarrow |5P_{3/2}, F=2\rangle$ transition. (C), A typical time-of-flight (TOF) image for atoms in 2D array of 1D tubes. (D), Normalized atom number $N(t)/N(0)$ versus dissipation-duration time t in log-linear plot for the dissipative dynamics of 1D quantum gas (blue diamonds) and 3D BEC (red circles). The solid curves are fittings using the stretched-exponential function, with the fitted stretched exponents $\alpha = 0.70(4)$ (blue) and $\alpha = 0.99(4)$ (red). This shows qualitative difference of the stretched-exponential decay versus the exponential one between strongly correlated one-dimensional gas and weakly interacting three-dimensional BEC. All error bars correspond to one standard deviation.

bosonic ^{87}Rb atoms trapped in a 1D array of tubes created by a two-dimensional (2D) optical lattice (see Supplementary materials (SM), and Fig. 1A). These atoms, initialized in the state of $|5S_{1/2}, F=1, m_F=1\rangle$, are confined in a crossed dipole trap and levitated against gravity using a magnetic field gradient. By adjusting the intensity of the lattice beams, we tune the lattice depth U_l of each lattice beam to modify the transverse ground state size a_{\perp} . This leads to the change of the 1D interaction strength $g_{1D} = 4\hbar^2 a_s / [m a_{\perp}^2 (1 - 1.46 \frac{a_s}{a_{\perp}})]$, where m is the mass of an atom, and a_s is the three-dimensional scattering length of ^{87}Rb at 98 Bohr radii. Thus, as we change the lattice depth U_l from 0.52 kHz to 430 kHz, the Luttinger liquid is tuned from weakly interacting region to Tonks-Girardeau region. The mean dimensionless interaction strength $\gamma = m g_{1D} / n \hbar^2$, representing the ratio of interaction energy and kinetic energy, is varied from 0.08 to 5.36, where n is the 1D atomic density. To introduce well-controlled one-body loss and avoid two-body loss caused by light-assisted collision, we set the frequency of the dissipation light to be 96 MHz blue-detuned from the transition of $|5S_{1/2}, F=1\rangle \rightarrow |5P_{3/2}, F=2\rangle$ (see Fig. 1B).

The loss introduced by such dissipation light leads to decay of the atom number in the Luttinger liquid. We fix the intensity of the dissipation light, and measure the residual atom number $N(t)$ with respect to the duration time t of the dissipation light. As shown in Fig. 1D, a decay process (blue diamonds) different from the conventional exponential decay is observed. Here, we set the lattice depth U_l to 65 kHz with a corresponding γ of 1.54, and fix the intensity of the dissipation light to a saturation parameter s of 0.01. In order to investigate this unconventional decay behavior, we fit the decay curve to

both stretched-exponential function and power function, and find the stretched-exponential function an obviously better fit. Inspired by Ref. [18], we use the fitting function

$$N(t) = N(0) \exp \left[- \left(\frac{t}{\tau_0} \right)^{\alpha} \right], \quad (1)$$

to extract stretched exponent α , dissipation characteristic time τ_0 , and initial atom number $N(0)$. $\alpha = 0.70 \pm 0.04$ and $\tau_0 = 25.3 \pm 1.1$ ms are obtained from fitting. For comparison, we also measure the loss dynamics of a three-dimensional Bose-Einstein condensate (BEC) in a crossed dipole trap where the decay follows an exponential function with the fitted stretched exponent $\alpha = 0.99 \pm 0.04$ (red circles in Fig. 1D).

Then, we change the dissipation rate in the Luttinger liquid by tuning the intensity of the dissipation light, so that the dissipation characteristic time τ_0 is ranged from 10 ms to 200 ms (Fig. 2A and B). At different dissipation rates, the atom number decay fittings show consistent stretched exponent α -s, remaining the same within one standard deviation (Fig. 2C). These data demonstrate that the stretched-exponential decay is a universal response of the Luttinger liquid to the dissipative probe. The stretched exponent α being independent of the dissipation strength, indicates that this exponent measures an intrinsic equilibrium property of the Luttinger liquid.

In order to explore the relation between the dissipative dynamics and the intrinsic correlations of the Luttinger liquid, we investigate how the stretched exponent α changes in different interaction regimes, tuning the Luttinger liquid from weakly interacting Bose gas to strongly correlated Tonks-Girardeau gas (Fig. 3A). Here, Luttinger liquid with the dimensionless interaction

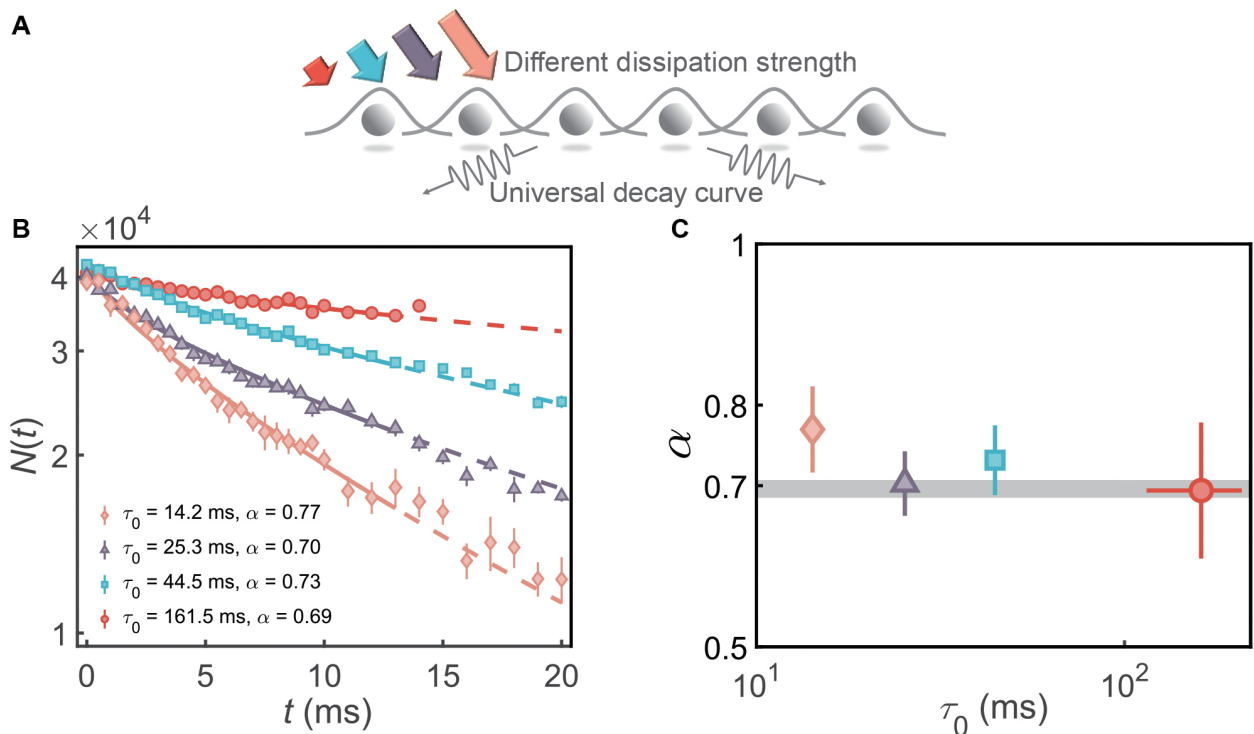


FIG. 2. **Dissipation dynamics at different dissipation strength for Luttinger liquid at dimensionless interaction strength $\gamma = 1.54$.** (A), Illustration of the dissipation process at different dissipation strength. Arrows with different colors imply different dissipation strengths applied to the 1D Bose gas. (B), The atom number $N(t)$ decays with respect to the dissipation time t in log-linear plot. Data with different labels represent dissipation processes at different dissipation strengths. The solid lines are fittings to the stretched-exponential decay in Eq. 1 using data within the upper bound of the dissipation time $t_u = 13$ ms. (C), The fitted α under different dissipation strength characterized by τ_0 . Vertical and horizontal error bars are the one standard deviations of the fitted α -s and τ_0 -s, respectively. The grey shade is the theoretical prediction of the non-Hermitian linear response theory, taking both finite-time correction and the atom-number inhomogeneity of different tubes into account. All error bars correspond to one standard deviation.

strength γ tuned from 0.08 to 5.36 are created, where we measure the atom decay curves (Fig. 3B), fit the data with Eq. 1, and extract the stretched exponent α from fittings at these dimensionless interaction strengths, as shown in Fig. 3C. Here, we obtain $\alpha = 0.93 \pm 0.16$, 0.77 ± 0.08 , 0.70 ± 0.04 , and 0.58 ± 0.06 for $\gamma = 0.08$, 0.72, 1.54, and 5.36, respectively.

These observations can be quantitatively understood by applying the non-Hermitian linear response theory to the Luttinger liquid [18, 21]. The theory connects dissipative dynamics of an observable to the correlation functions of the initial equilibrium state. By calculating the linear-order perturbations and spectral functions at zero temperature (see SM), the theoretical model predicts a stretched-exponential behavior for one-body dissipation as $N(t) \propto \exp[-(t/\tau_0)^{2\eta-1}]$. This prediction connects the stretched exponent α with the anomalous dimension η as $\alpha = 2\eta - 1$, where η is determined by Luttinger parameter K as $\eta = 1 - 1/(4K)$. Using Lieb-Liniger model, both η and K are determined by the dimensionless interaction strength γ (see SM). In Fig. 3C, we plot the theoretical predicted values for zero-temperature case

of $\alpha = 2\eta - 1$ versus γ (black solid curve). As the dimensionless interaction strength γ increases, the quantum fluctuations get stronger, and the quasi-particle description fails. This leads to a decreasing anomalous dimension η with a stronger deviation from 1, and a smaller Luttinger parameter K . This zero-temperature theoretical prediction curve is not fully aligned with experimental data due to the finite-time effect, because it is only valid at dissipation time $t \ll h/\pi k_B T$, where $h/\pi k_B T \sim 3$ ms for a typical temperature $T = 5$ nK (see SM). However, to guarantee reasonable data quality, experimentally we have to choose an intermediate dissipation time $t \sim h/\pi k_B T$, and the fitted stretched exponent α is influenced by the chosen upper bound t_u of the dissipation time (see Fig. S2B). Therefore, we extend the zero-temperature linear response theory into the finite-temperature regime with higher-order corrections, and plot the corrected theoretical curve of α in Fig. 3C (black dashed curve) and Fig. 2C (grey shade). For the fittings to extract α , we only include the experimental data within t_u , represented by the solid lines in both Fig. 2B and 3B. The corrected theoretical predic-

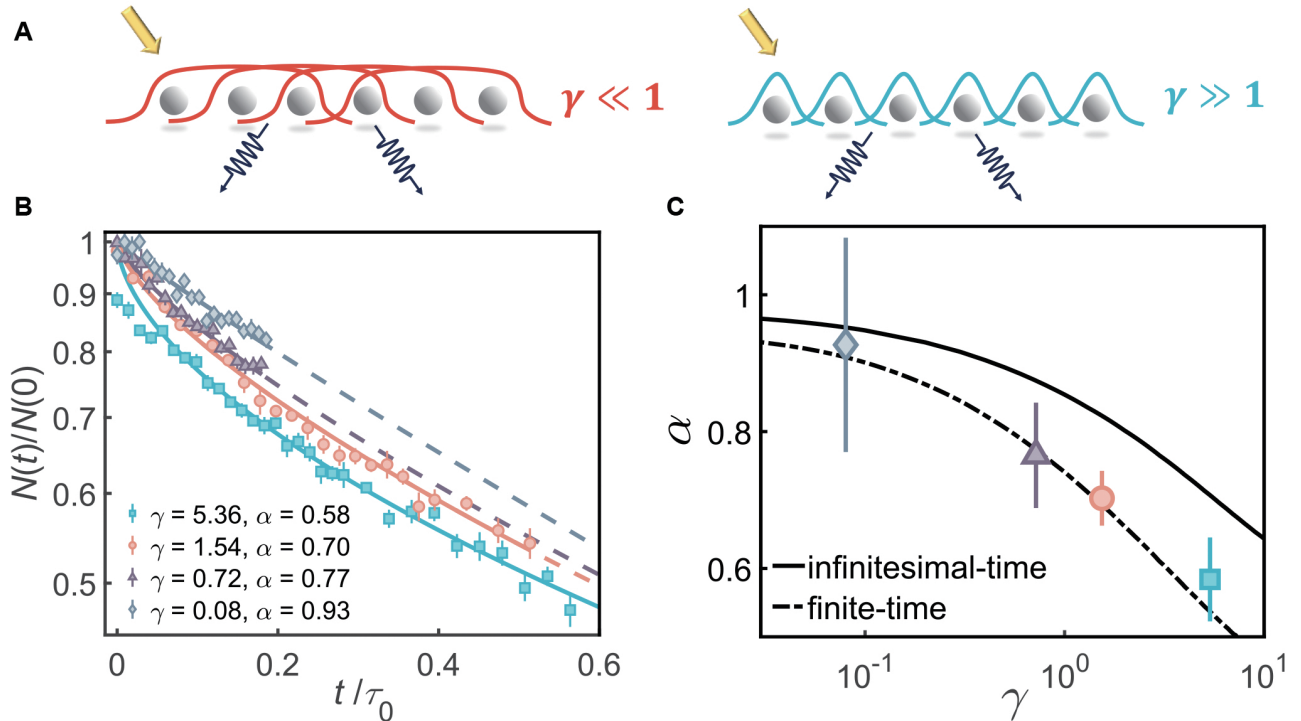


FIG. 3. **Dissipation dynamics at different dimensionless interaction strength γ .** (A), Illustration of the dissipation process at different dimensionless interaction strength γ . (B), The normalized atom number $N(t)/N(0)$ versus the rescaled time t/τ_0 at different γ in log-linear plot. Different labels show dissipation processes under different γ and the solid lines are fits to Eq. 1 using data within the upper bound of the dissipation time t_u . (C), The fitted stretched exponent α as a function of γ in linear-log plot. The black solid line shows the zero-temperature theoretical prediction for $\alpha = 2\eta - 1$ at different γ , while the dashed line shows the prediction with the finite-time correction. The grey diamonds with $\gamma = 0.08$ are in the crossover of the three-dimensional and the one-dimensional Bose gas region, and the theoretical prediction based on Lieb-Liniger model is not applicable to these data. All error bars correspond to one standard deviation.

tions agree well with our experimental data. One important thing to be noticed is that this finite-time correction is temperature-independent. We choose the interrogate time upper bound t_u to be inversely proportional to the temperature T of the system to keep the product of t_u and T as a constant (see SM).

To further demonstrate the universal dissipation dynamics is robust against the temperature variation and thermal effects, we perform the measurements for Luttinger Liquid with the same γ but different temperature T (Fig. 4A). To achieve this, we vary the depth of the crossed dipole trap while simultaneously adjust the depth of the lattice, to keep the dimensionless interaction strength γ constant at 1.63 ± 0.10 . As a result, we are able to tune the initial temperature of the ensemble from 5.6 nK to 16.4 nK (see SM for temperature calibration), and show consistent α values for different temperatures (Fig. 4C). We also rescale the dissipation time with the dissipation characteristic time τ_0 for data at each temperature, normalize the atom number, and find that the different temperature groups fall on the same line with $\alpha = 0.69$, which agrees well with the theoretical prediction of α at $\gamma = 1.63$ (Fig. 4B). This observation demon-

strates the universality of the dissipation process among a wide range of temperature. For each parameter set, we calculate the chemical potential of 1D tubes using the Yang-Yang equation [28], confirming that the chemical potential and the temperature are small enough compared with the tightly confined vibrational frequency and thus all ensembles can be described by one-dimensional Luttinger liquid.

In addition, we normalize the temperature T with the degenerate temperature $T_d = \hbar^2 n^2 / 2mk_B$, and plot α versus this normalized temperature in Fig. 4C inset. According to the theoretical prediction of the Lieb-Liniger model at finite temperature [39, 40], the normalized temperature T/T_d characterizes the extent of deformation in the spectral function caused by thermal effects. When T/T_d is smaller than 1.5, the spectral function remains almost unchanged compared with the zero-temperature case. Notably, our finite temperature results agree with this theoretical prediction, since the stretched exponent α , characterizing the spectral function, remains constant when T/T_d falls within the range of 0.6 to 1.6.

Our experiment demonstrates a universal dissipative dynamics in strongly correlated quantum gas, while the

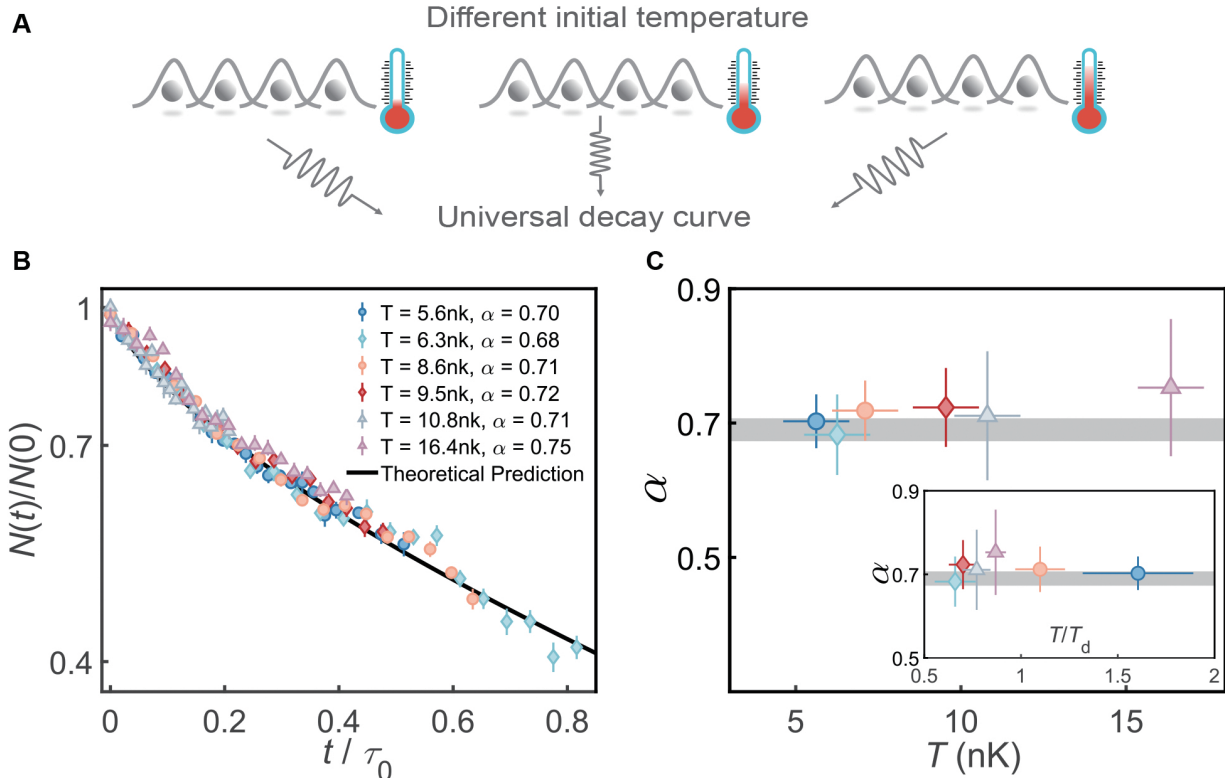


FIG. 4. **Dissipation dynamics at different temperature.** (A), Illustration of the dissipation processes at different temperature T . (B), The normalized atom number $N(t)/N(0)$ versus the rescaled dissipation time t/τ_0 in log-linear plot at different temperature. All data fall on the same stretched-exponential curve with $\alpha = 0.69$. All error bars correspond to one standard deviation. (C), Fitted α at different temperatures. The horizontal error bars stand for the uncertainty of the temperature, while the vertical error bars represent the one-standard-deviation confidence intervals of the fittings. The grey shade is estimated by the non-Hermitian linear response theory with the finite-time correction and the atom-number inhomogeneity. The inset shows the fitted α versus the rescaled temperature T/T_d , where $T_d = \hbar^2 n^2 / 2mk_B$.

dissipative process is only decided by the intrinsic correlations, independent of any external parameters such as dissipation strength and temperature. Similar phenomenon named anomalous decay of coherence was also observed in the superfluid-Mott insulator phase transition [41]. Such anomalous decay was attributed to the diffusion dynamics in momentum space in the original paper, and later explained by the non-Hermitian linear response theory [18]. In this article, we fully benchmark the unconventional decay behavior in 1D Bose gas experimentally, and show that the predictions of the non-Hermitian linear response theory agree well quantitatively with the experimental results. These results fully support the validity of this new theory, and extend this theory from zero temperature region to finite temperature region.

To conclude, we demonstrate a powerful method to utilize dissipation to probe quantum systems and observe equilibrium many-body quantum correlations. This novel dissipative probe method is used to detect the anomalous dimension in 1D Bose gas experimentally,

which is hardly accessible in a closed system due to technical difficulties [36]. This method is also expected to detect other quantum correlation features in strongly correlated systems with fractional excitations, including anomalous dimensions in one-dimensional Hubbard model with spin-charge separation and Fermi arc in high-TC superconductors.

Acknowledgement We acknowledge the inspiring discussions with H. Zhai, X.-W. Guan, and T. Giamarchi, and the technical supports from W. Zhang and Z. Zhang. **Funding:** This work is supported by National Natural Science Foundation of China (92165203, 61975092, 11974202, 12174358), National Key Research and Development Program of China (2021YFA1400904, 2021YFA0718303, 2022YFA1405300), Beijing Natural Science Foundation (Z180013) and Swiss National Science Foundation (200020-188687).

-
- * These authors contribute equally to this work.
† hujiazhong01@ultracold.cn
‡ ychen@giscaep.ac.cn
§ cwllaser@ultracold.cn
- [1] S Diehl, A Micheli, A Kantian, B Kraus, H P Büchler, and P Zoller, “Quantum states and phases in driven open quantum systems with cold atoms,” *Nat. Phys.* **4**, 878–883 (2008).
 - [2] Heinz-Peter Breuer, Elsi-Mari Laine, Jyrki Piilo, and Bassano Vacchini, “Colloquium: Non-Markovian dynamics in open quantum systems,” *Rev. Mod. Phys.* **88**, 021002 (2016).
 - [3] Yuto Ashida, Zongping Gong, and Masahito Ueda, “Non-Hermitian physics,” *Advances in Physics* **69**, 249–435 (2020).
 - [4] Emil J. Bergholtz, Jan Carl Budich, and Flore K. Kunst, “Exceptional topology of non-Hermitian systems,” *Rev. Mod. Phys.* **93**, 015005 (2021).
 - [5] Julian Léonard, Andrea Morales, Philip Zupancic, Tilman Esslinger, and Tobias Donner, “Supersolid formation in a quantum gas breaking a continuous translational symmetry,” *Nature* **543**, 87–90 (2017).
 - [6] Ruichao Ma, Brendan Saxberg, Clai Owens, Nelson Leung, Yao Lu, Jonathan Simon, and David I. Schuster, “A dissipatively stabilized Mott insulator of photons,” *Nature* **566**, 51–57 (2019).
 - [7] Giovanni Ferioli, Antoine Glicenstein, Igor Ferrier-Barbut, and Antoine Browaeys, “A non-equilibrium superradiant phase transition in free space,” *Nature Physics* (2023), 10.1038/s41567-023-02064-w.
 - [8] Lena H Dogra, Gevorg Martirosyan, Timon A Hilker, Jake AP Glidden, Jiří Etrych, Alec Cao, Christoph Eigen, Robert P Smith, and Zoran Hadzibabic, “Universal equation of state for wave turbulence in a quantum gas,” *Nature*, 1–4 (2023).
 - [9] S. Inouye, A.P. Chikkatur, D.M. Stamper-Kurn, J. Stenger, D.E. Pritchard, and W. Ketterle, “Superradiant Rayleigh Scattering from a Bose-Einstein,” *Science* **285**, 571–575 (1999).
 - [10] Kristian Baumann, Christine Guerlin, Ferdinand Brennecke, and Tilman Esslinger, “Dicke quantum phase transition with a superfluid gas in an optical cavity,” *Nature* **464**, 1301–1306 (2010).
 - [11] Xiaotian Zhang, Yu Chen, Zemao Wu, Juan Wang, Jijie Fan, Shujin Deng, and Haibin Wu, “Observation of a superradiant quantum phase transition in an intracavity degenerate fermi gas,” *Science* **373**, 1359–1362 (2021).
 - [12] Hideki Konishi, Kevin Roux, Victor Helsen, and Jean-Philippe Brantut, “Universal pair polaritons in a strongly interacting Fermi gas,” *Nature* **596**, 509–513 (2021).
 - [13] Yu-Kun Lu, Yair Margalit, and Wolfgang Ketterle, “Bosonic stimulation of atom–light scattering in an ultracold gas,” *Nat. Phys.* **19**, 210–214 (2023).
 - [14] Hans Keßler, Phatthamon Kongkhambut, Christoph Georges, Ludwig Mathey, Jayson G. Cosme, and Andreas Hemmerich, “Observation of a Dissipative Time Crystal,” *Phys. Rev. Lett.* **127**, 043602 (2021).
 - [15] Phatthamon Kongkhambut, Jim Skulte, Ludwig Mathey, Jayson G. Cosme, Andreas Hemmerich, and Hans Keßler, “Observation of a continuous time crystal,” *Science* **377**, 670–673 (2022).
 - [16] Y. Lin, J.P. Gaebler, F. Reiter, T.R. Tan, R. Bowler, A.S. Sørensen, D. Leibfried, and D.J. Wineland, “Dissipative production of a maximally entangled steady state of two quantum bits,” *Nature* **504**, 415–418 (2013).
 - [17] Hanna Krauter, Christine A. Muschik, Kasper Jensen, Wojciech Wasilewski, Jonas M. Petersen, J. Ignacio Cirac, and Eugene S. Polzik, “Entanglement Generated by Dissipation and Steady State Entanglement of Two Macroscopic Objects,” *Phys. Rev. Lett.* **107**, 080503 (2011).
 - [18] Lei Pan, Xin Chen, Yu Chen, and Hui Zhai, “Non-Hermitian linear response theory,” *Nat. Phys.* **16**, 767–771 (2020).
 - [19] Subir Sachdev, *Quantum phase transitions*. 2 ed. (Cambridge University Press, 2011).
 - [20] Thierry Giamarchi, *Quantum physics in one dimension* (Oxford University Press, 2003).
 - [21] Yu-Zhu Jiang, Yang-Yang Chen, and Xi-Wen Guan, “Understanding many-body physics in one dimension from the Lieb-Liniger model,” *Chin. Phys. B* **24**, 050311 (2015).
 - [22] Libo Liang, Wei Zheng, Ruixiao Yao, Qinpei Zheng, Zhiyuan Yao, Tian-Gang Zhou, Qi Huang, Zhongchi Zhang, Jilai Ye, Xiaoji Zhou, Xuzong Chen, Wenlan Chen, Hui Zhai, and Jiazong Hu, “Probing quantum many-body correlations by universal ramping dynamics,” *Science Bulletin* **67**, 2550–2556 (2022).
 - [23] Toshiya Kinoshita, Trevor Wenger, and David S Weiss, “Observation of a one-dimensional Tonks-Girardeau gas,” *Science* **305**, 1125–1128 (2004).
 - [24] Belén Paredes, Artur Widera, Valentin Murg, Olaf Mandel, Simon Fölling, Ignacio Cirac, Gora V Shlyapnikov, Theodor W Hänsch, and Immanuel Bloch, “Tonks-Girardeau gas of ultracold atoms in an optical lattice,” *Nature* **429**, 277–281 (2004).
 - [25] Elmar Haller, Mattias Gustavsson, Manfred J. Mark, Johann G. Danzl, Russell Hart, Guido Pupillo, and Hanns-Christoph Nägerl, “Realization of an excited, strongly correlated quantum gas phase,” *Science* **325**, 1224–1227 (2009).
 - [26] Elmar Haller, Russell Hart, Manfred J Mark, Johann G Danzl, Lukas Reichsöllner, Mattias Gustavsson, Marcello Dalmonte, Guido Pupillo, and Hanns-Christoph Nägerl, “Pinning quantum phase transition for a Luttinger liquid of strongly interacting bosons,” *Nature* **466**, 597–600 (2010).
 - [27] Florian Meinert, Michael Knap, Emil Kirilov, Katharina Jag-Lauber, Mikhail B. Zvonarev, Eugene Demler, and Hanns-Christoph Nägerl, “Bloch oscillations in the absence of a lattice,” *Science* **356**, 945–948 (2017).
 - [28] Bing Yang, Yang-Yang Chen, Yong-Guang Zheng, Hui Sun, Han-Ning Dai, Xi-Wen Guan, Zhen-Sheng Yuan, and Jian-Wei Pan, “Quantum criticality and the Tomonaga-Luttinger liquid in one-dimensional Bose gases,” *Phys. Rev. Lett.* **119**, 165701 (2017).
 - [29] Sebastian Erne, Robert Bücker, Thomas Gasenzer, Jürgen Berges, and Jörg Schmiedmayer, “Universal dynamics in an isolated one-dimensional Bose gas far from equilibrium,” *Nature* **563**, 225–229 (2018).
 - [30] Joshua M. Wilson, Neel Malvania, Yuan Le, Yicheng Zhang, Marcos Rigol, and David S. Weiss, “Observation of dynamical fermionization,” *Science* **367**, 1461–1464 (2020).
 - [31] Jayadev Vijayan, Pimonpan Sompert, Guillaume Sa-

- lomon, Joannis Koepsell, Sarah Hirthe, Annabelle Bohrdt, Fabian Grusdt, Immanuel Bloch, and Christian Gross, “Time-resolved observation of spin-charge deconfinement in fermionic hubbard chains,” *Science* **367**, 186–189 (2020).
- [32] Ruwan Senaratne, Danyel Cavazos-Cavazos, Sheng Wang, Feng He, Ya-Ting Chang, Aashish Kafle, Han Pu, Xi-Wen Guan, and Randall G Hulet, “Spin-charge separation in a one-dimensional Fermi gas with tunable interactions,” *Science* **376**, 1305–1308 (2022).
- [33] Jun Hui See Toh, Katherine C McCormick, Xinxin Tang, Ying Su, Xi-Wang Luo, Chuanwei Zhang, and Subhadeep Gupta, “Many-body dynamical delocalization in a kicked one-dimensional ultracold gas,” *Nature Physics* **18**, 1297–1301 (2022).
- [34] Yuan Le, Yicheng Zhang, Sarang Gopalakrishnan, Marcos Rigol, and David S Weiss, “Observation of hydrodynamization and local prethermalization in 1D Bose gases,” *Nature* **618**, 494–499 (2023).
- [35] Danyel Cavazos-Cavazos, Ruwan Senaratne, Aashish Kafle, and Randall G. Hulet, “Thermal disruption of a luttinger liquid,” *Nature Communications* **14**, 3154 (2023).
- [36] Yanliang Guo, Hepeng Yao, Sudipta Dar, Lorenzo Pizzino, Horvath Milena, Thierry Giamarchi, Manuele Landini, and Hanns-Christoph Nägerl, “Precise thermometer for low dimensional bosons,” (2023), [arXiv:arXiv:2308.04144](https://arxiv.org/abs/2308.04144).
- [37] Hepeng Yao, Lorenzo Pizzino, and Thierry Giamarchi, “Strongly-interacting bosons at 2D-1D dimensional crossover,” (2022), [arXiv:2204.02240](https://arxiv.org/abs/2204.02240).
- [38] Thomas Kohlert, Sebastian Scherg, Xiao Li, Henrik P. Lüschen, Sankar Das Sarma, Immanuel Bloch, and Monika Aidelsburger, “Observation of many-body localization in a one-dimensional system with a single-particle mobility edge,” *Phys. Rev. Lett.* **122**, 170403 (2019).
- [39] Song Cheng, Yang-Yang Chen, Xi-Wen Guan, Wen-Li Yang, and Hai-Qing Lin, “One-body dynamical correlation function of Lieb-Liniger model at finite temperature,” (2022), [arXiv:2211.00282](https://arxiv.org/abs/2211.00282).
- [40] Song Cheng, Yang-Yang Chen, Xi-Wen Guan, Wen-Li Yang, Rubem Mondaini, and Hai-Qing Lin, “Exact Spectral Function of One-Dimensional Bose Gases,” (2022), [arXiv:2209.15221](https://arxiv.org/abs/2209.15221).
- [41] Raphaël Bouganne, Manel Bosch Aguilera, Alexis Ghermaoui, Jérôme Beugnon, and Fabrice Gerbier, “Anomalous decay of coherence in a dissipative many-body system,” *Nat. Phys.* **16**, 21–25 (2020).

Supplementary Materials for **Observation of universal dissipative dynamics in strongly correlated quantum gas**

Yajuan Zhao,^{1†} Ye Tian,^{1†} Jilai Ye,^{1†} Yue Wu,² Zihan Zhao,¹ Zhihao Chi,¹
Tian Tian,¹ Hepeng Yao,³ Jiazhong Hu,^{1,4*} Yu Chen,^{5*} Wenlan Chen,^{1,4*}

¹Department of Physics and State Key Laboratory of Low Dimensional Quantum Physics,
Tsinghua University, Beijing, 100084, China

²Institute for Advanced Study, Tsinghua University, Beijing, 100084, China

³DQMP, University of Geneva, 24 Quai Ernest-Ansermet, CH-1211 Geneva, Switzerland

⁴Frontier Science Center for Quantum Information and Collaborative Innovation
Center of Quantum Matter, Beijing, 100084, China

⁵Graduate School of China Academy of Engineering Physics, Beijing, 100193, China

†These authors contribute equally to this work.

*To whom correspondence should be addressed; E-mail: hujiazhong01@ultracold.cn,
ychen@gscaep.ac.cn, cwllaser@ultracold.cn.

September 20, 2023

Materials and Methods

Preparation of Luttinger liquid

We start with a Bose-Einstein condensate (BEC) of $N = 4 \times 10^4$ ^{87}Rb atoms at $|5S_{1/2}, F = 1, m_F = 1\rangle$, confined in a horizontally crossed dipole trap with a wavelength at 1064 nm. The waist of each dipole beam is $50 \mu\text{m}$ and the angle between them is 45° , which induces an anisotropic 3D harmonic trap. The trap depth is $U_z/h = 6.8$ kHz in total and its vibrational frequencies along three dimensions are $\omega_x = 2\pi \times 19.3$ Hz, $\omega_y = 2\pi \times 13.5$ Hz, and $\omega_z = 2\pi \times 33.0$ Hz respectively. Meanwhile, we introduce a magnetic field gradient at 30.7 Gauss/cm to compensate for the gravity. The BEC is then transformed into 1D Luttinger liquid by adiabatically ramping up a 2D optical lattice with a wavelength of 776.5 nm within 80 ms. These two lattice beams propagate perpendicularly to each other, with horizontal and vertical polarization respectively and frequency difference at 160 MHz so that the interference between lattice beams can be avoided. The waist of the lattice beams is $400 \mu\text{m}$, much larger than the atomic cloud size, to guarantee the homogeneity of radial vibrational frequency ω_\perp among the ensemble. The 2D optical lattice, together with the crossed dipole trap, provides independent control of the radial and axial confinements of the 1D gas.

Non-Hermitian linear response theory on Luttinger liquids

When a 1D system experiences a dissipative perturbation formed as $-i\kappa\hat{O}^\dagger(z, t)\hat{O}(z, t)$ starting from the initial time $t_i = 0$ with κ denoting the dissipation rate, any observable \hat{W} will have a measurable difference $\delta\mathcal{W}(t)$ at time t compared with its value at the steady state without dissipation. $\delta\mathcal{W}(t)$ is expressed as

$$\delta\mathcal{W}(t) = 2\kappa \int dz \int_0^t d\tau \langle \hat{O}^\dagger(z, \tau) \hat{W}(t) \hat{O}(z, \tau) - \frac{1}{2} \{ \hat{O}(z, \tau) \hat{O}(z, \tau), \hat{W}(t) \} \rangle, \quad (1)$$

where $\{, \}$ is the anti-commutator. To describe one-body loss in our experiment, we use $\hat{O}(z) =$

$\int dk \hat{a}_k e^{ikz}$ where \hat{a}_k is the bosonic annihilation operator at momentum mode k , and we choose the atom number $\hat{\mathcal{W}} = \hat{n}_k = \hat{a}_k^\dagger \hat{a}_k$ as the observable. Following the derivations in Ref (18), Eq. 1 becomes

$$\delta n_k(t) = -2\kappa n_k(0) \int_0^t d\tau g_k(\tau) g_k(-\tau), \quad (2)$$

where $g_k(t)$ is the single-particle correlation function in the form of $g_k(t) = \langle [\hat{a}_k(t), \hat{a}_k^\dagger(0)] \rangle$. When the 1D system is described by the Luttinger liquid theory at zero temperature, the single-particle correlation function is dominant by the phase fluctuations and $g_k(t)$ has a form of $g_k(t) \sim t^{\eta-1}$, where η is the anomalous dimension with $\eta = 1 - 1/(4K)$. Here, K is the Luttinger parameter and can be uniquely determined by the dimensionless interaction strength γ (see supplementary text). Although $g_k(t)$ has weak dependence on momentum k , leading to k -dependent $\delta n_k(t)$, these k -dependent deviations from $t^{\eta-1}$ cancel each other when we integrate the whole momentum space. Consequently, the total atom number $N(t)$ decays in the form

$$N(t) = N(0) \exp[-(t/\tau_0)^{2\eta-1}], \quad (3)$$

where τ_0 is a time constant. When the dimensionless interaction strength γ in the Luttinger liquid increases, the anomalous dimension η decreases. This leads to a smaller stretched exponent in the decay curve, deviating further from the conventional exponential decay. More detailed discussions and derivations can be found in the supplementary text.

It is worth noting that this theory has an upper limit and a lower limit for the time scale within which it could accurately describe the dissipation dynamics in 1D Bose gas. The upper bound of the timescale is on the order of tens of $1/\kappa$, and the extremely-short-timescale dynamics is determined by high-frequency spectral function, where linear Luttinger liquid approximation fails to be exact. Besides, the theoretical prediction fails when the dimensionless interaction strength becomes too small, because the system is no longer in the Tomonaga-Luttinger liquid

(TLL) regime in this case.

Finite-time corrections at finite temperature

When the system has a finite temperature T , the dynamics of the total atom number in Eq. 3 needs to be corrected into the following form (see supplementary text)

$$N(t) = N(0) \exp \left\{ - \frac{1}{\tau_0^{2\eta-1}} \int_0^t d\tau \left[\frac{h}{\pi k_B T} \times \sinh \left(\frac{\pi k_B T \tau}{h} \right) \right]^{2\eta-2} \right\}. \quad (4)$$

Therefore the stretched-exponential form in Eq. 3 is only valid when $\pi k_B T t / h \ll 1$. In our experiment, this requires $t \ll h / \pi k_B T \sim 3$ ms for a typical temperature at $T = 5$ nK. Due to the measurement noise, experimentally we need to choose an intermediate dissipation duration time $t \sim h / \pi k_B T$, so a correction to the stretched exponent in the case of zero temperature is necessary. Practically, we set an upper bound t_u of the dissipation time, to satisfy $\pi k_B T t_u / h = 5$. In other words, we keep $t_u T$ constant at $\mathcal{C} = 5h / \pi k_B$ in the fittings of decay curves to extract the stretched exponent. The constant \mathcal{C} is chosen to guarantee that the atom number difference between Eq. 3 and Eq. 4 is within 6%, comparable to the error bar of the measured atom number in our data. In Fig. 2B and Fig. 3B, the boundary between the solid lines and the dashed lines represents t_u . Then, by fitting the curve in Eq. 4 with a stretched-exponential function $\exp \left[-(t/\tau_0)^{\alpha^*} \right]$ within t_u , we are able to extract a corrected theoretical prediction for the stretched exponent α^* , which takes the finite-time effect into account, and is only determined by the dimensionless interaction strength γ and the constant $\mathcal{C} = t_u T$. The α^* -s are shown in the black dashed line in Fig. 3C, and grey shades in Fig. 2C and Fig. 4C.

Thermometer for 1D Bose gas

We calibrate the temperature of the 1D bosonic system accurately based on the one-body correlation function $g^{(1)}(z, z') = \langle \hat{\Psi}^\dagger(z') \hat{\Psi}(z) \rangle$, according to the method in Ref. (36). Due to

the strong quantum fluctuations in one dimension, the decay of $g^{(1)}$ has a significant dependence on temperature, which allows us to use it as a thermometer. On the one hand, by performing the Fourier transform of the momentum distribution obtained through TOF measurement, we get integrated correlation function $G^{(1)}(z) = \int dz' g^{(1)}(z' + z, z')$ for our 1D Bose gas. On the other hand, we can use the ab-initio quantum Monte Carlo (QMC) method to simulate the Lieb-Liniger Hamiltonian

$$H_{LL} = \sum_i \left[-\frac{\hbar^2}{2m} \frac{\partial^2}{\partial z_i^2} + V(z_i) \right] + g_{1D} \sum_{i < j} \delta(z_i - z_j), \quad (5)$$

with i and j span the set of particles, g_{1D} the coupling constant and $V(z_j)$ the harmonic trap, similar to Refs. (37,42). Our simulation is performed for a system with weighted averaged atom number $\bar{N} = \sum_{p,q} N_{p,q}^2 / \sum_{p,q} N_{p,q}$ where $N_{p,q}$ is the atom number of the tube on site labelled by p, q . Thanks to the worm algorithm implementation (43), we can compute $G^{(1)}(z)$ at different values of temperature which serves as a ruler. By comparing the experimental data with the QMC results, we can determine the temperature of the system within a resolution of 1 nK. The numerical calculations make use of the ALPS scheduler library and statistical analysis tools (44–46).

Supplementary Text

Lieb-Liniger model in a harmonic trap

Here we use the Lieb-Liniger Hamiltonian (47) in a harmonic trap at zero temperature to describe the atoms in each 1D tube:

$$H_{LL} = \sum_i \left\{ -\frac{\hbar^2}{2m} \frac{\partial^2}{\partial z_i^2} + V(z_i) \right\} + \sum_{i < j} g_{1D} \delta(z_i - z_j), \quad (6)$$

where $V(z) = \frac{1}{2}m\omega^2 z^2$ is a harmonic potential along the z direction with ω denoting the vibrational frequency. Using the Bethe ansatz and local density approximation, this model can

be analytically solved and we can calculate the equilibrium state at zero temperature. For each position z , we define the local dimensionless interaction strength $\gamma(z) = mg_{1\text{D}}/n_{1\text{D}}(z)\hbar^2$ (48) where $n_{1\text{D}}(z)$ is the local 1D density. Following the local density approximation, we define a cutoff radius R_c , where $n_{1\text{D}}(z)$ equals to zero for any $|z| > R_c$. Therefore, we define the average dimensionless interaction strength of one tube as

$$\gamma = \frac{\int_{-R_c}^{R_c} dz n_{1\text{D}}(z) \gamma(z)}{\int_{-R_c}^{R_c} dz n_{1\text{D}}(z)}. \quad (7)$$

In our experiment, we load atoms into about 3300 tubes of the 2D optical lattice, and each tube contains an ensemble of 1D Bose gas. Here the atom number in each tube is calculated by the density distribution of the initial BEC in the harmonic trap while the total atom number is 4×10^4 . Therefore, the atom number $N_{p,q}$ can be calculated according to the Thomas-Fermi approximation as

$$N_{p,q} = N_{0,0} \left[1 - \frac{(pa)^2}{R_x^2} - \frac{(qa)^2}{R_y^2} \right], \quad (8)$$

where p and q are integers and label the 2D lattice sites in the x - y plane, $a = 388.25$ nm is the lattice constant, $N_{0,0}$ is the atom number in the central tube, and R_x and R_y are the Thomas-Fermi radii which can be calculated according to the trap geometries. Then we calculate the mean atom number per tube \bar{N} by

$$\bar{N} = \frac{\sum_{p,q} N_{p,q}^2}{\sum_{p,q} N_{p,q}}, \quad (9)$$

and the averaged interaction strength $\bar{\gamma}$ to characterize the 1D system

$$\bar{\gamma} = \frac{\int_{-R_c}^{R_c} dz \bar{n}_{1\text{D}}(z) \bar{\gamma}(z)}{\bar{N}}, \quad (10)$$

where $\bar{n}_{1\text{D}}(z)$ is the density distribution of a tube with \bar{N} atoms and $\bar{\gamma}(z) = mg_{1\text{D}}/\bar{n}_{1\text{D}}(z)\hbar^2$.

For each tube, there is a stretched-exponential decay of the atom number under its γ . To include the inhomogeneity of the atom number distribution theoretically in the theoretical simulations, we sum up each stretched-exponential decay according to its atom number and then

fit it with an overall stretched-exponential function $N_0 \exp[-(t/\tau_0)^\alpha]$. Under this method, the stretched exponent α is consistent with the predicted α by the averaged interaction strength $\bar{\gamma}$ under the Lieb-Liniger model. Therefore, in Fig. 2C, Fig. 3C, and Fig. 4C, we use the α obtained by this method to include the inhomogeneity of the atom number as the theoretical predicted value, and the grey shades in the plots represent one standard deviations of fittings.

Luttinger parameter K , anomalous dimension η , and interaction strength γ

In this section, we will derive the relation between the Luttinger parameter K , the anomalous dimension η , and the interaction strength γ . The low-energy physics of the 1D gas can be described by the effective field theory, and the effective Hamiltonian (20) is

$$\hat{H}_{\text{eff}} = \int dz \left[\frac{\pi v_s K}{2\hbar} \hat{\Pi}^2 + \frac{\hbar v_s}{2\pi K} (\partial_z \hat{\phi})^2 \right], \quad (11)$$

under the long-wavelength limit. Here $\hat{\phi}$ is the field operator and $\hat{\Pi}$ is the canonical momentum of $\hat{\phi}$. As bosonic operators, $\hat{\phi}$ and $\hat{\Pi}$ obey the bosonic commutation relation. The coefficient K here is the Luttinger parameter and v_s is the sound velocity. According to this Hamiltonian, the single-particle spectral function $\mathcal{A}_k(\omega)$ of 1D gas is proportional to $(\omega^2 - \Delta_k^2)^{-\eta} \Theta(\omega^2 - \Delta_k^2)$ where $\Theta(x)$ is the heaviside step function and η is the anomalous dimension, and η is related to K by $\eta = 1 - 1/(4K)$.

By applying Bethe ansatz solutions (47, 49), we can calculate the Luttinger parameter K . Based on the solutions, the energy of each particle at zero temperature is

$$\epsilon(n) = \frac{\hbar^2 n^2}{2m} e(\gamma), \quad (12)$$

where n is the mean density of 1D gas and $\gamma = mg_{1D}/n\hbar^2$ is the interaction strength, and the function $e(\gamma)$ is determined by

$$e(\gamma) = \frac{\gamma^3}{\lambda^3(\gamma)} \int_{-1}^1 g(z, \gamma) z^2 dz. \quad (13)$$

Here the functions $g(z, \gamma)$ and $\lambda(\gamma)$ are calculated through the Bethe ansatz solutions

$$g(z, \gamma) = \frac{1}{2\pi} \int_{-1}^1 \frac{2\lambda(\gamma)}{\lambda^2(\gamma) + (y-z)^2} g(y, \gamma) dy + \frac{1}{2\pi}, \quad (14)$$

$$\lambda(\gamma) = \gamma \int_{-1}^1 g(z, \gamma) dz. \quad (15)$$

In these equations, the only free parameter is the dimensionless interaction strength γ . Therefore, once it is determined, Eq. 12 to Eq. 15 can be solved numerically. Based on these, the Luttinger parameter K is obtained explicitly as a function of γ as

$$K = \frac{\pi}{\sqrt{3e(\gamma) - 2\gamma \frac{de(\gamma)}{d\gamma} + \frac{1}{2}\gamma^2 \frac{d^2e(\gamma)}{d\gamma^2}}}. \quad (16)$$

Now we move to the finite-temperature regime, and we want to prove that the Luttinger parameter K is almost unchanged at finite temperatures. We use the Yang-Yang equation to calculate this model at finite temperatures. The Luttinger parameter K is calculated as $K = v_s/v_n$, where $v_s = \sqrt{(\partial^2 F/\partial L^2)L^2/mn}$ is the sound velocity and $v_n = \partial^2 F/\partial N^2(2L/h)$ is the density stiffness. Here n is the 1D density, L is the system's length, N is the total atom number, and F is the free energy from the Yang-Yang equation.

By introducing a dimensionless universal function $\tilde{f}(\gamma, \tilde{T})$ which is similar to $e(\gamma)$, we write out the total free energy as

$$F = N \frac{\hbar^2 n^2}{2m} \tilde{f}(\gamma, \tilde{T}), \quad (17)$$

where $\tilde{T} = 2mk_B T/\hbar^2 n^2$ is the dimensionless temperature. It is intuitive to see that $\tilde{f}(\gamma, \tilde{T})$ becomes $e(\gamma)$ when \tilde{T} approaches to zero. Therefore, we obtain the explicit formula of the finite-temperature Luttinger parameter K as

$$K = \frac{\pi}{\sqrt{3\tilde{f} - 2\gamma \frac{\partial \tilde{f}}{\partial \gamma} + \frac{1}{2}\gamma^2 \frac{\partial^2 \tilde{f}}{\partial \gamma^2} + 4\gamma \tilde{T} \frac{\partial^2 \tilde{f}}{\partial \gamma \partial \tilde{T}} + 4\tilde{T}^2 \frac{\partial^2 \tilde{f}}{\partial \tilde{T}^2}}}. \quad (18)$$

In order to calculate $\tilde{f}(\gamma, \tilde{T})$, we need to solve the self-consistent Yang-Yang equations as follows,

$$F = \frac{N}{n} \int_{-\infty}^{\infty} \left(\frac{\hbar^2 k^2}{2m} - \varepsilon(k) \right) \rho(k) dk - \frac{N k_B T}{n} \int_{-\infty}^{\infty} dk f(k) \log \left(1 + e^{-\frac{\varepsilon(k)}{k_B T}} \right), \quad (19)$$

$$2\pi \rho(k) = \frac{1}{1 + e^{\varepsilon(k)/k_B T}} \left(1 + 2g_{1D} \int_{-\infty}^{\infty} dq \frac{\rho(q)}{\frac{m}{\hbar^2} g_{1D}^2 + \frac{\hbar^2 (k-q)^2}{m}} \right), \quad (20)$$

$$\varepsilon(k) = -\mu + \frac{\hbar^2 k^2}{2m} - \frac{k_B T g_{1D}}{\pi} \int_{-\infty}^{\infty} dq \frac{\log(1 + e^{-\varepsilon(k)/k_B T})}{\frac{m}{\hbar^2} g_{1D}^2 + \frac{\hbar^2 (k-q)^2}{m}}, \quad (21)$$

$$\mu = \frac{1}{n} \int_{-\infty}^{\infty} \left(\frac{\hbar^2 k^2}{2m} - \varepsilon(k) \right) \rho(k) dk + \frac{k_B T}{n} \int_{-\infty}^{\infty} dq \left(\frac{1}{2\pi} - f(q) \right) \log(1 + e^{-\varepsilon(k)/k_B T}), \quad (22)$$

$$f(k) = \rho(k) (1 + e^{\varepsilon(k)/k_B T}). \quad (23)$$

Combining Eq. 19 to Eq. 23, we calculate $\tilde{f}(\gamma, \tilde{T})$ and the Luttinger parameter K at finite temperature. In fig. S1, we show that K is almost unchanged under the finite-temperature effects.

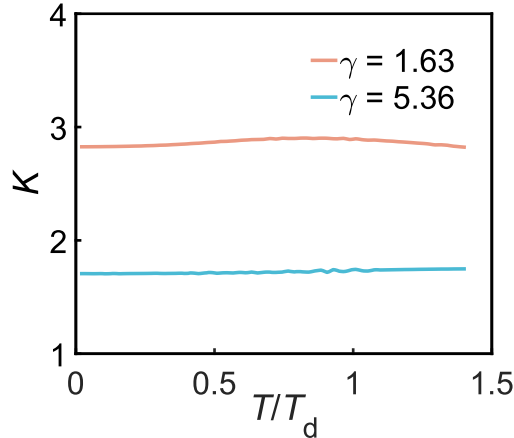


Fig. S1. Dependence of Luttinger parameter on temperature. The Luttinger parameter K versus the rescaled temperature T/T_d , with $T_d = \hbar^2 n^2 / 2m k_B$ denoting the degenerate temperature. Different colors represent different dimensionless interaction strengths γ .

Non-Hermitian linear response theory at finite temperature

For a quantum system experiencing a dissipative perturbation, the dissipation term \hat{H}_{diss} can be written as a non-Hermitian Hamiltonian with Langevin noise operators in the form of

$$\hat{H}_{\text{diss}} = -i\kappa\hat{O}^\dagger\hat{O} + \hat{O}^\dagger\xi + \xi^\dagger\hat{O}. \quad (24)$$

Here ξ and ξ^\dagger are the Langevin noise operators, and κ denotes the dissipation rate. Therefore, for any observable \hat{W} , we consider the difference $\delta\mathcal{W}(t)$ at time t compared with its value at the steady state without dissipation. The form of $\delta\mathcal{W}(t)$ is then calculated as

$$\delta\mathcal{W}(t) = 2\kappa \int \mathbf{d}z \int_0^t \mathbf{d}\tau \langle \hat{O}^\dagger(z, \tau) \hat{W}(t) \hat{O}(z, \tau) - \frac{1}{2} \{ \hat{O}(z, \tau) \hat{O}(z, \tau), \hat{W}(t) \} \rangle, \quad (25)$$

where $\{, \}$ corresponds to the anti-commutator. To describe the one-body loss in our experiment, we use $\hat{O}(z) = \int dk \hat{a}_k e^{ikz}$ where \hat{a}_k is the bosonic annihilation operator at momentum k mode, and we choose the atom number operator of momentum k mode $\hat{n}_k = \hat{a}_k^\dagger \hat{a}_k$ as the observable \hat{W} . Then we obtain

$$\delta n_k(t) = -2\kappa n_k(0) \int_0^t \mathbf{d}\tau g_k(\tau) g_k(-\tau), \quad (26)$$

$$n_k(t) = n_k(0) e^{-\mathcal{F}_k(t)}, \quad (27)$$

$$\mathcal{F}_k(t) = 2\kappa \int_0^t \mathbf{d}\tau g_k(\tau) g_k(-\tau), \quad (28)$$

here $g_k(t)$ is the single-particle correlation function formed as

$$g_k(t) = \langle [\hat{a}_k(t), \hat{a}_k^\dagger(0)] \rangle = \int \mathbf{d}\omega \mathcal{A}_k(\omega) e^{i\omega t}, \quad (29)$$

where $\mathcal{A}_k(\omega)$ is the single-particle spectral function defined in the previous section. By integrating Eq. 29, we find

$$g_k(t) \approx c_0 |t|^{\eta-1} \cos(\Delta_k t), \quad (30)$$

where c_0 is a constant. Therefore, $\mathcal{F}_k(t)$ has a form as

$$\begin{aligned}\mathcal{F}_k(t) &= \kappa \frac{c_0^2}{2} \int_0^t d\tau \tau^{2\eta-2} [1 + \cos(2\Delta_k \tau)] \\ &= (t/\tau_0)^{2\eta-1} + G(2\Delta_k t),\end{aligned}\quad (31)$$

where $\tau_0^{1-2\eta} = \kappa c_0^2/2$, and $G(2\Delta_k t)$ is a very small oscillation function whose period is π/Δ_k . The major contribution term $(t/\tau_0)^{2\eta-1}$ in $\mathcal{F}_k(t)$ is the momentum- k independent. Therefore, this leads to $n_k(t) = n_k(0) \exp[-(t/\tau_0)^{2\eta-1}]$, and the total atom number $N(t)$ also follows the same form as,

$$N(t) = \sum_k n_k(t) = N(0) \exp[-(t/\tau_0)^{2\eta-1}]. \quad (32)$$

The oscillation terms $G(2\Delta_k t)$ cancel each other because the oscillation frequencies $2\Delta_k$ are different. This is quite remarkable that the momentum average in presence of the trap indeed helps the emergence of universal behavior in $N(t)$.

For finite-temperature corrections, we need to consider the spectral function at non-zero temperature. When the Luttinger liquid approximation is still valid in the Lieb-Liniger model, the single-particle correlation function is obtained by a conformal transformation which sends $t - z/v_s = z^*$ to $e^{i2\pi z^*/h\beta}$ and $\bar{z}^* = t + z/v_s$ to $e^{i2\pi \bar{z}^*/h\beta}$, and $\beta = 1/k_B T$ is the inverse temperature, where k_B is the Boltzmann constant. Then the spatial correlation function becomes

$$g(z, t; 0, 0) = \left| \left(\frac{\pi}{h\beta} \right)^2 \frac{1}{\sinh(\pi z^*/h\beta) \sinh(\pi \bar{z}^*/h\beta)} \right|^{1-\eta} \Theta(t^2 - z^2/v_s^2). \quad (33)$$

Then the single-particle correlation function at finite temperature $g_k(t, T)$ is calculated as

$$\begin{aligned}g_k(t, T) &= \int_{-v_s|t|}^{v_s|t|} dz e^{ikz} g(z, t) \\ &= \int_{-v_s|t|}^{v_s|t|} dz \frac{e^{ikz} \left(\frac{\pi}{h\beta} \right)^{2(\eta-1)}}{\left| \sinh^2 \left(\frac{\pi t}{h\beta} \right) - \sinh^2 \left(\frac{\pi z}{h\beta v_s} \right) \right|^{1-\eta}} \\ &\approx \int dz \frac{e^{ikz}}{\left| \frac{h^2 \beta^2}{\pi^2} \sinh^2 \left(\frac{\pi t}{h\beta} \right) - \frac{z^2}{v_s^2} \right|^{1-\eta}}\end{aligned}$$

$$= g_k \left(\frac{h\beta}{\pi} \sinh \left(\frac{\pi t}{h\beta} \right), 0 \right). \quad (34)$$

Because here we focus on the short-time correlation function, we have the approximation $\sinh(\pi z/h\beta v_s)h\beta/\pi \approx z/v_s$ in the integration region. In the last line of the above equation, $g_k(t, 0)$ is obtained from the Fourier transformation from the space-time side. Therefore, the correlation function $g_k(t, T)$ at finite temperature T can be approximately obtained by transformation $t \rightarrow \sinh(\pi t/h\beta)h\beta/\pi$ from the zero-temperature correlation function. Therefore, we have

$$g_k(t) \approx c_0 \left| \frac{h\beta}{\pi} \sinh \left(\frac{\pi t}{h\beta} \right) \right|^{-\eta} \cos \left[\Delta_k \frac{h\beta}{\pi} \sinh \left(\frac{\pi t}{h\beta} \right) \right]. \quad (35)$$

Then $\mathcal{F}_k(t)$ is calculated as

$$\mathcal{F}_k(t) = \frac{1}{\tau_0^{2\eta-1}} \int_0^t d\tau \left(\sinh \frac{\pi\tau}{h\beta} \right)^{2\eta-2} \left(\frac{h\beta}{\pi} \right)^{2\eta-2}. \quad (36)$$

Then $N(t)$ follows a modified decay form as

$$N(t) = N(0) \exp \left[-\frac{1}{\tau_0^{2\eta-1}} \int_0^t d\tau \left(\sinh \frac{\pi\tau}{h\beta} \right)^{2\eta-2} \left(\frac{h\beta}{\pi} \right)^{2\eta-2} \right]. \quad (37)$$

Only when $t \ll h\beta/\pi$ is satisfied, $N(t)$ will have the same form as the result at zero temperature. Due to technical noises in the experiment, we have to choose $\pi t/h\beta \sim 1$. Therefore, we interrogate the time duration from 0 to t_u to check the dissipative dynamics of $N(t)$. For $t \in [0, t_u]$, we fit $N(t)$ with the stretched-exponential function $N(0) \exp \left[-(t/\tau_0')^{\alpha^*} \right]$, and we expect α^* becomes $2\eta - 1$ when t_u approaches to zero. In fig. S2A, we first plot the exact $N(t)$ for both zero temperature (yellow curve) and finite one (cyan curve), then also plot the fitted function $N(0) \exp \left[-(t/\tau_0')^{\alpha^*} \right]$ for comparison (red curve) where we set $t^* = \pi t_u/h\beta = 4.8$ as the same one in the main text. It shows a good consistency between the finite-temperature curve $N(t)$ and the fitted one. In fig. S2B, we plot α^* versus t^* for different η (or γ).

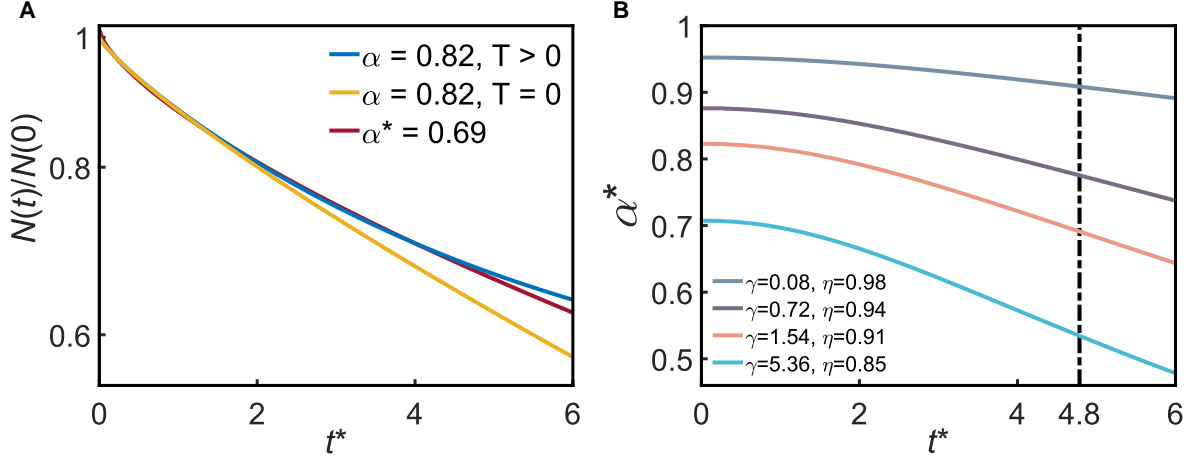


Fig. S2. Finite-time correction. (A) The cyan line is the dissipation curve in the form of Eq. 37 with $\eta = 0.91$. The yellow line is the dissipation curve with the same $\eta = 0.91$ but at zero temperature formed in Eq. 32. Here, t^* is the rescaled dissipation time $t^* = \pi k_B T t / h$. When we use the stretched-exponential function $N(0) \exp[-(t/\tau_0')^{\alpha^*}]$ to fit the cyan line, the red line gives $\alpha^* = 0.69$ when we set the time upper bound at $t^* = 4.8$. Here the y axis is in a logarithmic scale and the x axis is in a linear scale. (B) For different γ or η , as the t^* increases, the fitted α^* decreases and the dashed line represents the t^* we use in our experiment.

References

1. S. Diehl, A. Micheli, A. Kantian, B. Kraus, H. P. Büchler, P. Zoller. Quantum states and phases in driven open quantum systems with cold atoms. Nat. Phys. **4**, 878–883 (2008).
2. H.-P. Breuer, E.-M. Laine, J. Piilo, B. Vacchini. Colloquium: Non-Markovian dynamics in open quantum systems. Rev. Mod. Phys. **88**, 021002 (2016).
3. Y. Ashida, Z. Gong, M. Ueda. Non-Hermitian physics. Advances in Physics **69**, 249–435 (2020).
4. E. J. Bergholtz, J. C. Budich, F. K. Kunst. Exceptional topology of non-Hermitian systems. Rev. Mod. Phys. **93**, 015005 (2021).
5. J. Léonard, A. Morales, P. Zupancic, T. Esslinger, T. Donner. Supersolid formation in a quantum gas breaking a continuous translational symmetry. Nature **543**, 87–90 (2017).
6. R. Ma, B. Saxberg, C. Owens, N. Leung, Y. Lu, J. Simon, D. I. Schuster. A dissipatively stabilized Mott insulator of photons. Nature **566**, 51–57 (2019).
7. G. Ferioli, A. Glicenstein, I. Ferrier-Barbut, A. Browaeys. A non-equilibrium superradiant phase transition in free space. Nature Physics (2023).
8. L. H. Dogra, G. Martirosyan, T. A. Hilker, J. A. P. Glidden, J. Etrych, A. Cao, C. Eigen, R. P. Smith, Z. Hadzibabic. Universal equation of state for wave turbulence in a quantum gas. Nature **620**, 521–524 (2023).
9. S. Inouye, A. Chikkatur, D. Stamper-Kurn, J. Stenger, D. Pritchard, W. Ketterle. Superradiant Rayleigh Scattering from a Bose-Einstein. Science **285**, 571–575 (1999).

10. K. Baumann, C. Guerlin, F. Brennecke, T. Esslinger. Dicke quantum phase transition with a superfluid gas in an optical cavity. Nature **464**, 1301–1306 (2010).
11. X. Zhang, Y. Chen, Z. Wu, J. Wang, J. Fan, S. Deng, H. Wu. Observation of a superradiant quantum phase transition in an intracavity degenerate fermi gas. Science **373**, 1359–1362 (2021).
12. H. Konishi, K. Roux, V. Helsen, J.-P. Brantut. Universal pair polaritons in a strongly interacting Fermi gas. Nature **596**, 509–513 (2021).
13. Y.-K. Lu, Y. Margalit, W. Ketterle. Bosonic stimulation of atom–light scattering in an ultracold gas. Nat. Phys. **19**, 210–214 (2023).
14. H. Keßler, P. Kongkhambut, C. Georges, L. Mathey, J. G. Cosme, A. Hemmerich. Observation of a Dissipative Time Crystal. Phys. Rev. Lett. **127**, 043602 (2021).
15. P. Kongkhambut, J. Skulte, L. Mathey, J. G. Cosme, A. Hemmerich, H. Keßler. Observation of a continuous time crystal. Science **377**, 670–673 (2022).
16. Y. Lin, J. Gaebler, F. Reiter, T. Tan, R. Bowler, A. Sørensen, D. Leibfried, D. Wineland. Dissipative production of a maximally entangled steady state of two quantum bits. Nature **504**, 415–418 (2013).
17. H. Krauter, C. A. Muschik, K. Jensen, W. Wasilewski, J. M. Petersen, J. I. Cirac, E. S. Polzik. Entanglement Generated by Dissipation and Steady State Entanglement of Two Macroscopic Objects. Phys. Rev. Lett. **107**, 080503 (2011).
18. L. Pan, X. Chen, Y. Chen, H. Zhai. Non-Hermitian linear response theory. Nat. Phys. **16**, 767–771 (2020).
19. S. Sachdev. Quantum phase transitions. 2 ed., (Cambridge University Press 2011).

20. T. Giamarchi. Quantum physics in one dimension, (Oxford University Press 2003).
21. Y.-Z. Jiang, Y.-Y. Chen, X.-W. Guan. Understanding many-body physics in one dimension from the Lieb-Liniger model. Chin. Phys. B **24**, 050311 (2015).
22. L. Liang, W. Zheng, R. Yao, Q. Zheng, Z. Yao, T.-G. Zhou, Q. Huang, Z. Zhang, J. Ye, X. Zhou, X. Chen, W. Chen, H. Zhai, J. Hu. Probing quantum many-body correlations by universal ramping dynamics. Science Bulletin **67**, 2550–2556 (2022).
23. T. Kinoshita, T. Wenger, D. S. Weiss. Observation of a one-dimensional Tonks-Girardeau gas. Science **305**, 1125–1128 (2004).
24. B. Paredes, A. Widera, V. Murg, O. Mandel, S. Fölling, I. Cirac, G. V. Shlyapnikov, T. W. Hänsch, I. Bloch. Tonks–Girardeau gas of ultracold atoms in an optical lattice. Nature **429**, 277–281 (2004).
25. E. Haller, M. Gustavsson, M. J. Mark, J. G. Danzl, R. Hart, G. Pupillo, H.-C. Nägerl. Realization of an excited, strongly correlated quantum gas phase. Science **325**, 1224–1227 (2009).
26. E. Haller, R. Hart, M. J. Mark, J. G. Danzl, L. Reichsöllner, M. Gustavsson, M. Dalmonte, G. Pupillo, H.-C. Nägerl. Pinning quantum phase transition for a Luttinger liquid of strongly interacting bosons. Nature **466**, 597–600 (2010).
27. F. Meinert, M. Knap, E. Kirilov, K. Jag-Lauber, M. B. Zvonarev, E. Demler, H.-C. Nägerl. Bloch oscillations in the absence of a lattice. Science **356**, 945–948 (2017).
28. B. Yang, Y.-Y. Chen, Y.-G. Zheng, H. Sun, H.-N. Dai, X.-W. Guan, Z.-S. Yuan, J.-W. Pan. Quantum criticality and the Tomonaga-Luttinger liquid in one-dimensional Bose gases. Phys. Rev. Lett. **119**, 165701 (2017).

29. S. Erne, R. Bücker, T. Gasenzer, J. Berges, J. Schmiedmayer. Universal dynamics in an isolated one-dimensional Bose gas far from equilibrium. Nature **563**, 225–229 (2018).
30. J. M. Wilson, N. Malvania, Y. Le, Y. Zhang, M. Rigol, D. S. Weiss. Observation of dynamical fermionization. Science **367**, 1461–1464 (2020).
31. J. Vijayan, P. Sompet, G. Salomon, J. Koepsell, S. Hirthe, A. Bohrdt, F. Grusdt, I. Bloch, C. Gross. Time-resolved observation of spin-charge deconfinement in fermionic hubbard chains. Science **367**, 186–189 (2020).
32. R. Senaratne, D. Cavazos-Cavazos, S. Wang, F. He, Y.-T. Chang, A. Kafle, H. Pu, X.-W. Guan, R. G. Hulet. Spin-charge separation in a one-dimensional Fermi gas with tunable interactions. Science **376**, 1305–1308 (2022).
33. J. H. See Toh, K. C. McCormick, X. Tang, Y. Su, X.-W. Luo, C. Zhang, S. Gupta. Many-body dynamical delocalization in a kicked one-dimensional ultracold gas. Nature Physics **18**, 1297–1301 (2022).
34. Y. Le, Y. Zhang, S. Gopalakrishnan, M. Rigol, D. S. Weiss. Observation of hydrodynamization and local prethermalization in 1D Bose gases. Nature **618**, 494–499 (2023).
35. D. Cavazos-Cavazos, R. Senaratne, A. Kafle, R. G. Hulet. Thermal disruption of a luttinger liquid. Nature Communications **14**, 3154 (2023).
36. Y. Guo, H. Yao, S. Dar, L. Pizzino, H. Milena, T. Giamarchi, M. Landini, H.-C. Nägerl. Precise thermometer for low dimensional bosons [arXiv:2308.04144](https://arxiv.org/abs/2308.04144) [cond-mat] (2023).
37. H. Yao, L. Pizzino, T. Giamarchi. Strongly-interacting bosons at 2D-1D dimensional crossover [arXiv:2204.02240](https://arxiv.org/abs/2204.02240) [cond-mat] (2022).

38. T. Kohlert, S. Scherg, X. Li, H. P. Lüschen, S. Das Sarma, I. Bloch, M. Aidelsburger. Observation of many-body localization in a one-dimensional system with single-particle mobility edge Phys. Rev. Lett. **122**, 170403 (2019).
39. S. Cheng, Y.-Y. Chen, X.-W. Guan, W.-L. Yang, H.-Q. Lin. One-body dynamical correlation function of Lieb-Liniger model at finite temperature `arXiv:2211.00282` [cond-mat] (2022).
40. S. Cheng, Y.-Y. Chen, X.-W. Guan, W.-L. Yang, R. Mondaini, H.-Q. Lin. Exact Spectral Function of One-Dimensional Bose Gases `arXiv:2209.15221` [cond-mat] (2022).
41. R. Bouganne, M. Bosch Aguilera, A. Ghermaoui, J. Beugnon, F. Gerbier. Anomalous decay of coherence in a dissipative many-body system. Nat. Phys. **16**, 21–25 (2020).
42. H. Yao, T. Giamarchi, L. Sanchez-Palencia. Lieb-Liniger bosons in a shallow quasiperiodic potential: Bose glass phase and fractal Mott lobes. Phys. Rev. Lett. **125**, 060401 (2020).
43. M. Boninsegni, N. Prokof'ev, B. Svistunov. Worm algorithm for continuous-space path integral Monte Carlo simulations. Phys. Rev. Lett. **96**, 070601 (2006).
44. M. Troyer, B. Ammon, E. Heeb. Parallel object oriented Monte Carlo Simulations. Lect. Notes Comput. Sci. **1505**, 191 (1998).
45. A. Albuquerque, F. Alet, P. Corboz, P. Dayal, A. Feiguin, S. Fuchs, L. Gamper, E. Gull, S. Gürtler, A. Honecker, R. Igarashi, M. Körner, A. Kozhevnikov, A. Läuchli, S. Manmana, M. Matsumoto, I. McCulloch, F. Michel, R. Noack, G. Pawłowski, L. Pollet, T. Pruschke, U. Schollwöck, S. Todo, S. Trebst, M. Troyer, P. Werner, S. Wessel. The ALPS project release 1.3: Open-source software for strongly correlated systems. J. Magn. Magn. Mater. **310**, 1187–1193. Proceedings of the 17th International Conference on Magnetism (2007).

46. B. Bauer, L. D. Carr, H. G. Evertz, A. Feiguin, J. Freire, S. Fuchs, L. Gamper, J. Gukelberger, E. Gull, S. Guertler, A. Hehn, R. Igarashi, S. V. Isakov, D. Koop, P. N. Ma, P. Mates, H. Matsuo, O. Parcollet, G. Pawłowski, J. D. Picon, L. Pollet, E. Santos, V. W. Scarola, U. Schollwöck, C. Silva, B. Surer, S. Todo, S. Trebst, M. Troyer, M. L. Wall, P. Werner, S. Wessel. The ALPS project release 2.0: open source software for strongly correlated systems. J. Stat. Mech. Theory Exp. **2011**, P05001 (2011).
47. E. H. Lieb, W. Liniger. Exact analysis of an interacting Bose gas. I. The general solution and the ground state. Phys. Rev. **130**, 1605 (1963).
48. V. Dunjko, V. Lorent, M. Olshanii. Bosons in cigar-shaped traps: Thomas-Fermi regime, Tonks-Girardeau regime, and in between. Phys. Rev. Lett. **86**, 5413 (2001).
49. Y.-Z. Jiang, Y.-Y. Chen, X.-W. Guan. Understanding many-body physics in one dimension from the Lieb-Liniger model. Chin. Phys. B **24**, 050311 (2015).